J. Plasma Fusion Res. SERIES, Vol.1 (1998) 468–471

Ideal and Resistive Stability of the TJ-II Heliac Device

GARCIA Luis*, SANCHEZ Raul and JIMENEZ Juan Antonio[1]
Universidad Carlos III, 28911 Leganés, Madrid, Spain
[1]Asociación EURATOM-CIEMAT, 28040 Madrid, Spain

(Received: 30 September 1997/Accepted: 22 October 1997)

Abstract

The magnetohydrodynamic (MHD) linear stability properties of the TJ-II heliac standard configuration [1] are examined by two different methods. The first method uses a local ballooning criterion derived for three-dimensional (3D) general configurations [2]. From the ideal limit of this criterion, a critical $<\beta> \sim 1.3\%$ is obtained. When resistivity and compressibility effects are included, unstable modes with $\gamma\tau_{hp} \sim 10^{-3}$ do not appear until β is close to the ideal critical limit. In the second method, the incompressible full MHD equations are solved for ideal or resistive modes. The latter method provides information about the spatial structure of the eigenfunction. Preliminary results for an ideally unstable β-value show modes with global character due to the low shear of the configuration.

Keywords:

stellarator, heliac, TJ-II, resistive MHD, ballooning modes, global modes

1. Introduction

Because of the complexity of the problem, MHD calculations in toroidal geometry are usually done with some simplifying assumptions. Since pressure-driven instabilities are a key feature in stellarators, criteria based on localized modes, like the Mercier criterion[3] or 3D ballooning criterion[2], are customarily employed to assess MHD stability properties in stellarators. The advantage of the ballooning formalism is its simplicity since it reduces the eigenvalue problem to a one-dimensional boundary-valued system of ordinary linear differential equations along the field line. This is very useful in order to make fast estimations of critical β-values, but does not provide information about the global structure of the eigenfunction. Up to now, the calculation of global modes has been based on formulations of the ideal MHD energy principle in magnetic coordinates[4, 5]. Here, we develop a formalism to solve the full MHD equations incompressibly for either ideal or resistive modes.

Ideal and resistive ballooning stability results for the TJ-II standard configuration are discussed in Section 2. The numerical formalism to solve the full MHD equations is presented in Sec. 3. Preliminary results for an ideally unstable TJ-II configuration are presented in Sec. 4. Finally, some conclusions are drawn in Sec. 5.

2. Ballooning Stability of TJ-II

The equations used to examine the ballooning stability in the TJ-II standard configuration are described in Ref. [6]. They are the 3D ballooning mode equations derived in Ref. [2] rewritten using magnetic Boozer coordinates (ρ, θ, ζ) [7].

The more unstable solutions are obtained when integration begins at $(\theta, \zeta) = (0, 0)$, since this is the point where curvature is most unfavorable. The numerical equilibria used throughout this work have been obtained using fixed [8] and free [9] boundary versions of the VMEC equilibrium code. The equilibrium pressure has been chosen linear in the normalized toroidal magnetic flux $s = \rho^2$, and the net current has been set to zero in all cases.

*Corresponding author's e-mail: lgarcia@fis.uc3m.es

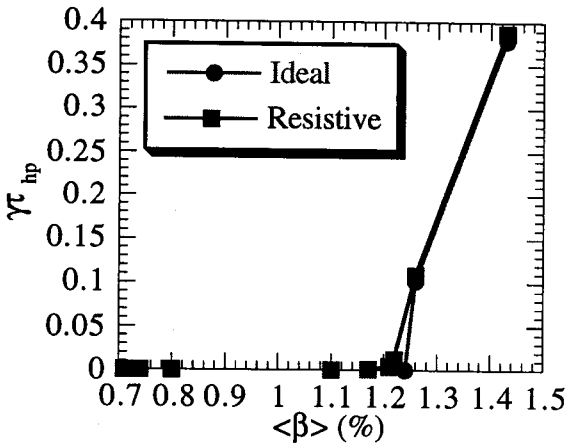

Fig. 1. Ideal and resistive compressible growth rate γ *vs.* $<\beta>$. We have set $m^2/S = 10^{-3}$.

Solving the ballooning equations for the standard TJ-II configuration we obtain that the most unstable modes accumulate at the outer surfaces. In the ideal limit, and for a series of fixed-boundary equilibria, we have obtained stability up to $<\beta> \sim 1.3\%$. Access to a second stability region seems to be found for higher-β equilibria. However, this stabilization disappears when free-boundary equilibria are employed. The fictitious stabilization is because, for high-β fixed-boundary equilibria, the last flux surfaces are squeezed against the fixed boundary, and support a fictitious extra magnetic pressure which makes ballooning stability to be overestimated[6].

In the pressure convection limit ($\Gamma = 0$, where Γ is the specific heats ratio), unstable resistive modes with rapidly decreasing growth rate γ are found for all β. When compressibility is included, the excitation of parallel sound waves stabilizes most of the modes predicted in the pressure convection limit. The growth rates for ideal and resistive compressible modes are plotted *vs.* β in Fig. 1 for $m^2/S = 10^{-3}$, where m is the poloidal mode number, $S = \tau_R/\tau_{hp}$ is the Lundquist number, $\tau_R = \mu_0 a^2/\eta$ is the resistive diffusion time, and $\tau_{hp} = R_0(\mu_0\rho_m)^{1/2}/B_0$ is the poloidal Alfvén time. It is observed that the ideal critical β is only slightly lowered due to resistive effects.

3. Incompressible MHD Equations

We begin with the usual incompressible MHD equations, namely

$$\frac{\partial \boldsymbol{A}}{\partial t} = -\nabla\alpha + \boldsymbol{v} + \boldsymbol{B} - \eta \boldsymbol{J}, \tag{1}$$

$$\rho_m\left(\frac{\partial \boldsymbol{v}}{\partial t} + \boldsymbol{v}\cdot\nabla\boldsymbol{v}\right) = -\nabla p + \boldsymbol{J}\times\boldsymbol{B}, \tag{2}$$

$$\frac{\partial p}{\partial t} + \boldsymbol{v}\cdot\nabla p = 0, \tag{3}$$

$$\boldsymbol{B} = \nabla\times\boldsymbol{A}, \tag{4}$$

$$\boldsymbol{v} = \nabla\times\boldsymbol{\Omega}, \tag{5}$$

where the magnetic field and the velocity are written in terms of the vector potentials since $\nabla\cdot\boldsymbol{B} = \nabla\cdot\boldsymbol{v} = 0$, α is the electrostatic potential, and the mass density ρ_m is assumed to be constant.

The MHD equations are solved in toroidal geometry, and we use magnetic Boozer coordinates [7] based on the equilibrium as coordinate system. The gauge for the potentials is chosen to be

$$A_\rho = \Omega_\rho = 0. \tag{6}$$

By taking the curl of the linear momentum balance equation multiplied by the jacobian, we obtain:

$$\frac{\partial \boldsymbol{U}}{\partial t} = -\sqrt{g}\nabla\sqrt{g}\times\nabla p + \sqrt{g}\nabla\times(\sqrt{g}\boldsymbol{J}\times\boldsymbol{B}), \tag{7}$$

where $\boldsymbol{U} = \rho_m\sqrt{g}\nabla\times(\sqrt{g}\boldsymbol{v})$.

With the preceding specifications and the definitions $A_\zeta = -\Psi$ (the poloidal magnetic flux function), $A_\theta = -\chi$ (the toroidal magnetic flux function), $\Omega_\zeta = -\Phi$ (the poloidal stream function), and $\Omega_\theta = -\Lambda$ (the toroidal stream function), the equations that are solved are (in dimensionless form):

$$\frac{\partial\Psi}{\partial t} = \frac{\partial\alpha}{\partial\zeta} - \frac{\rho t}{\sqrt{g}}\left(\frac{1}{\rho}\frac{\partial\Phi}{\partial\theta} - \frac{\partial\Lambda}{\partial\zeta}\right) + \eta J_\zeta. \tag{8}$$

$$\frac{\partial\chi}{\partial t} = \frac{1}{\rho}\frac{\partial\alpha}{\partial\theta} - \frac{1}{\sqrt{g}}\left(\frac{1}{\rho}\frac{\partial\Phi}{\partial\theta} - \frac{\partial\Lambda}{\partial\zeta}\right) + \eta J_\theta, \tag{9}$$

$$0 = -\frac{\partial\alpha}{\partial\rho} + \frac{1}{\sqrt{g}}\left[\frac{\partial\Phi}{\partial\rho} - \iota\frac{\partial(\rho\Lambda)}{\partial\rho}\right] - \eta J_\rho, \tag{10}$$

$$\frac{\partial U^\theta}{\partial t} = S^2\frac{\beta_0}{2\varepsilon^2}\left(\frac{\partial\sqrt{g}}{\partial\rho}\frac{\partial p}{\partial\zeta} - \frac{\partial\sqrt{g}}{\partial\zeta}\frac{\partial p}{\partial\rho}\right) + S^2\left\{\frac{\partial}{\partial\zeta}[g(J^\theta B^\zeta - J^\zeta B^\theta)] - \frac{\partial}{\partial\rho}[g(J^\rho B^\theta - J^\theta B^\rho)]\right\}, \tag{11}$$

$$\frac{\partial U^\zeta}{\partial t} = S^2\frac{\beta_0}{2\varepsilon^2}\left(\frac{1}{\rho}\frac{\partial\sqrt{g}}{\partial\theta}\frac{\partial p}{\partial\rho} - \frac{\partial\sqrt{g}}{\partial\rho}\frac{1}{\rho}\frac{\partial p}{\partial\theta}\right) + S^2\left\{\frac{1}{\rho}\frac{\partial}{\partial\rho}[\rho g(J^\zeta B^\rho - J^\rho B^\zeta)] - \frac{1}{\rho}\frac{\partial}{\partial\theta}[g(J^\theta B^\zeta - J^\zeta B^\theta)]\right\}, \tag{12}$$

$$\frac{\partial p}{\partial t} = \frac{\mathrm{d}p_{eq}}{\mathrm{d}\rho}\frac{1}{\sqrt{g}}\left(\frac{1}{\rho}\frac{\partial\Phi}{\partial\theta} - \frac{\partial\Lambda}{\partial\zeta}\right), \tag{13}$$

where

$$J^{\rho}=\frac{1}{\sqrt{g}}\left(\frac{1}{\rho}\frac{\partial B_{\zeta}}{\partial\theta}-\frac{\partial B_{\theta}}{\partial\zeta}\right),$$

$$J^{\theta}=\frac{1}{\sqrt{g}}\left(\frac{\partial B_{\rho}}{\partial\zeta}-\frac{\partial B_{\zeta}}{\partial\rho}\right),$$

$$J^{\zeta}=\frac{1}{\sqrt{g}}\left[\frac{1}{\rho}\frac{\partial(\rho B_{\theta})}{\partial\rho}-\frac{1}{\rho}\frac{\partial B_{\rho}}{\partial\theta}\right], \tag{14}$$

$$B^{\rho}=\frac{1}{\sqrt{g}}\left(\frac{\partial\chi}{\partial\zeta}-\frac{1}{\rho}\frac{\partial\Psi}{\partial\theta}\right), \quad B^{\theta}=\frac{1}{\sqrt{g}}\frac{\partial\Psi}{\partial\rho},$$

$$B^{\zeta}=-\frac{1}{\sqrt{g}}\frac{1}{\rho}\frac{\partial(\rho\chi)}{\partial\rho}, \tag{15}$$

$$U^{\theta}=\frac{\partial}{\partial\zeta}(\sqrt{g}v_{\rho})-\frac{\partial}{\partial\rho}(\sqrt{g}v_{\zeta}),$$

$$U^{\zeta}=\frac{1}{\rho}\frac{\partial}{\partial\rho}(\rho\sqrt{g}v_{\theta})-\frac{1}{\rho}\frac{\partial}{\partial\theta}(\rho\sqrt{g}v_{\rho}), \tag{16}$$

$$v^{\rho}=\frac{1}{\sqrt{g}}\left(\frac{\partial\Lambda}{\partial\zeta}-\frac{1}{\rho}\frac{\partial\Phi}{\partial\theta}\right), \quad v^{\theta}=\frac{1}{\sqrt{g}}\frac{\partial\Phi}{\partial\rho},$$

$$v^{\zeta}=-\frac{1}{\sqrt{g}}\frac{1}{\rho}\frac{\partial(\rho\Lambda)}{\partial\rho}. \tag{17}$$

In Eqs. (8)–(17), all lengths are normalized to the minor radius a, the resisitivity and the pressure to their equilibrium value at the magnetic axis, the magnetic field to the vacuum field at the magnetic axis, and the time to the resistive diffusion time τ_R.

We assume a perfect conducting wall boundary condition at the plasma edge ($\rho = 1$). This implies the following boundary conditions:

$$B^{\rho}(1)=v^{\rho}(1)=\alpha(1)=p(1)=0. \tag{18}$$

To solve Eqs. (8)–(13), the perturbed quantities are expanded in Fourier series in the generalized poloidal and toroidal angles. The equations are time-advanced using the numerical method described in Refs. [10, 11] for tokamaks. The problem is now more complex due to the coupling of different toroidal mode numbers since the equilibrium contains not only $n = 0$ but all the multiples of the number of field periods.

4. Global Stability of TJ-II

We now apply the numerical scheme described in the previous section to an equilibrium of the standard configuration of TJ-II with $<\beta> = 1.43\%$. This case is ideal ballooning unstable with a growth rate $\gamma\tau_{hp} \sim 0.7$ at the very edge. Since TJ-II has four field periods, there are three different mode families generated by the beating of equilibrium and perturbation [5]: they correspond to $n = 0, 4, 8, \ldots$, $n = 2, 6, 10, \ldots$, and $n = 1, 3, 5, \ldots$. The rotational transform of the chosen configuration is such that the Fourier component with the lowest n-value and its rational surface inside the plasma is ($m = 5$, $n = 7$). For this reason, we have concentrated in the study of the family with odd n-values.

Since no net toroidal current flows in the plasma, the only source of free energy for the instability is the pressure gradient in the bad curvature region. The first two terms in the *r.h.s.* of Eqs. (11) and (12) coupled to the pressure equation (13) can drive the instability. On the other hand, the remaining terms in the *r.h.s.* of Eqs. (11) and (12) correspond to the field-line bending and are stabilizing. In Fig. 2, we plot the dominant components of the jacobian for the equilibrium considered.

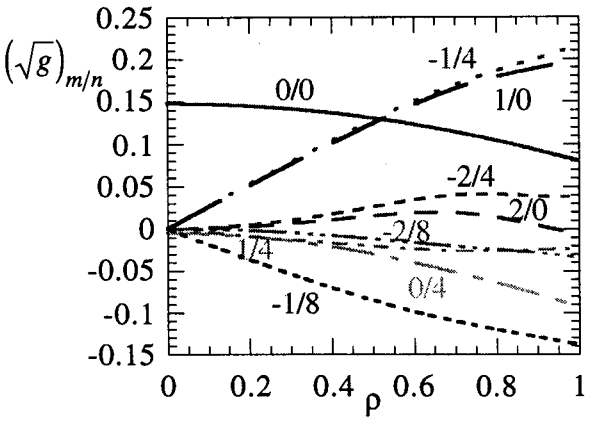

Fig. 2. Dominant components of the jacobian for the configuration with $<\beta> = 1.43\%$. For the 0/0 component, we represent its value minus 1.

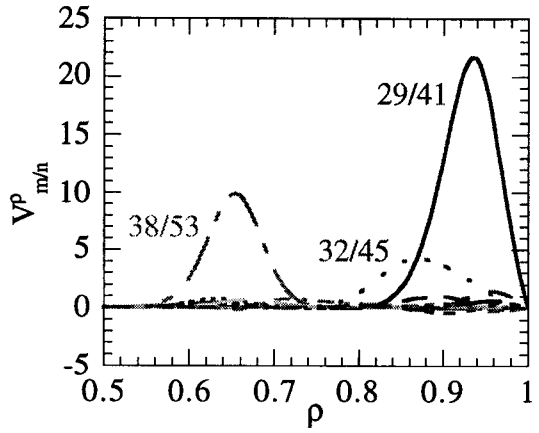

Fig. 3. Dominant components of the eigenfunction *vs.* radius when n = 37, 41, 45, 49, 53 are included in the calculation.

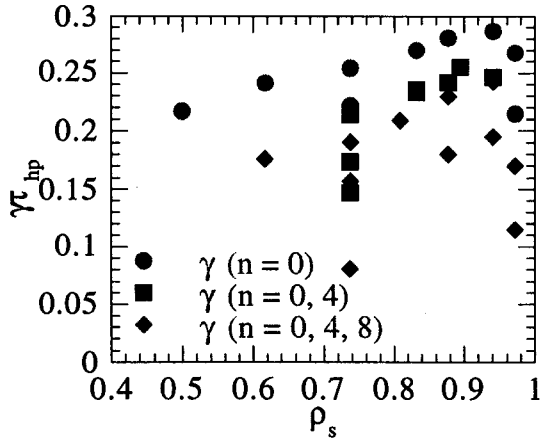

Fig. 4. Growth rate *vs.* radial position of the dominant component's rational surface.

To study the stability properties of the mode family, we have first calculated the stability of all odd n-values from 7 to 51 with some Fourier component resonant in the plasma taking only $n = 0$ components for the equilibrium. Afterwards, we have included $n = 4$, and $n = 8$ equilibrium components for each of the cases in order to get convergence for the growth rate. The spectrum is converged in each of these calculations with the kinetic energy falling six orders of magnitude. We show in Fig. 3 the radial dependence of the dominant components when $n = 37, 41, 45, 49, 53$ are included in the calculation. The mode has a global character and is not localized in radius. Finally, the values obtained for the growth rates are plotted in Fig. 4. They are represented versus the position of the dominant component's rational surface. As can be seen, the growth rate decreases with the number of couplings, and the more unstable modes are located in the outer part of the plasma. It is apparent that the family growth rate (normalized to poloidal Alfvén time) is smaller than 0.25.

5. Conclusion

We have examined the MHD linear stability properties of the TJ-II heliac standard configuration using two different approaches. The local ballooning criterion gives an ideal limit of $<\beta> \sim 1.3\%$. This limit is only slightly lowered when resistivity and compressibility effects are included. By solving the incompressible full MHD equations, we have found that the modes have a global character, and the value of the growth rate is reduced with respect to the maximum value obtained with the local ballooning criterion.

Acknowledgments

We are very grateful to S.P. Hirshman for providing us with the VMEC code. This work was done under financial support from DGES Project No. PB93-0231-C02-01.

References

[1] C. Alejaldre *et al.*, Fusion Tech. **17**, 131 (1990).
[2] D. Correa-Restrepo, Zeits. Naturf. **37a**, 848 (1982).
[3] C. Mercier, Nucl. Fusion **1**, 47 (1960).
[4] D.V. Anderson, W.A. Cooper, U. Schwenn and R. Gruber, in *Proceedings, Joint Varenna-Lausanne International Workshop on Theory of Fusion Plasmas* (Compositori, Bologna, 1988), p. 93.
[5] C. Schwab, Phys. Fluids B **5**, 3195 (1993).
[6] R. Sanchez, J.A. Jimenez, L. Garcia and A. Varias, Nucl. Fusion **37**, 1363 (1997).
[7] A.H. Boozer, Phys. Fluids **23**, 904 (1980).
[8] S.P. Hirshman, O.J. Betancourt, J. Compt. Phys. **96**, 99 (1991).
[9] S.P. Hirshman, W.I. van Rij and P. Merkel, Compt. Phys. Comm. **43**, 143 (1986).
[10] L.A. Charlton, J.A. Holmes, H.R. Hicks, V.E. Lynch and B.A. Carreras, J. Compt. Phys. **63**, 107 (1986).
[11] L.A. Charlton, J.A. Holmes, V.E. Lynch, B.A. Carreras and T.C. Hender, J. Compt. Phys. **86**, 270 (1990).